https://doi.org/10.5194/egusphere-2023-1167
Preprint. Discussion started: 19 July 2023

Optimizing maximum carboxylation rate for North America's boreal forests in the Canadian Land Surface Scheme Including Biogeochemical Cycles (CLASSIC) v.1.3

Bo Qu[1,2,3], Alexandre Roy[2,3], Joe R. Melton[4], Jennifer L. Baltzer[5], Youngryel Ryu[6], Matteo Detto[7], Oliver Sonnentag[1,2]

[1] Département de géographie, Université de Montréal, Montréal, QC H2V 0B3, Canada
[2] Centre d'Études Nordiques, Université Laval, Québec, QC G1V 0A6, Canada
[3] Centre de recherche sur les interactions bassins versants-écosystèmes aquatiques (RIVE), Université du Québec à Trois-Rivières, Trois-Rivières, QC G8Z 4M3, Canada
[4] Climate Research Division, Environment and Climate Change Canada, Victoria, BC V8W 2Y2, Canada
[5] Biology Department, Wilfrid Laurier University, Waterloo, ON N2L 3C5, Canada
[6] Department of Landscape Architecture and Rural Systems Engineering, College of Agriculture and Life Sciences, Seoul National University, Seoul 08826, Republic of Korea
[7] Department of Ecology and Evolutionary Biology, Princeton University, Princeton, NJ 08544, USA

Correspondence to: Bo Qu (bo.qu@umontreal.ca)

Abstract. The maximum carboxylation rate (V_{cmax}) is an important parameter for the coupled simulation of gross primary production (GPP) and evapotranspiration (ET) in terrestrial biosphere models (TBMs) such as the Canadian Land Surface Scheme Including biogeochemical Cycles (CLASSIC). Observations of V_{cmax} show it to vary both spatially and temporally, but it is often prescribed as constant in time and space for plant functional types (PFTs) in TBMs, which introduces large errors over North America's boreal biome. To reduce this uncertainty, we used a Bayesian algorithm to optimize V_{cmax25} (V_{cmax} at 25 °C) in CLASSIC against eddy covariance observations at eight mature boreal forest stands in North America for six representative PFTs (two trees, two shrubs, and two herbs). As expected, the simulated GPP and ET using the optimized parameters generally obtained reduced root mean square deviation values compared with eddy covariance observations and corresponding stand-level estimates obtained from gridded global data products. The optimized V_{cmax25} values for each PFT compared reasonably well with reported estimates derived from leaf-level gas exchange measurements. However, a large spatial variability of V_{cmax25} was identified, especially for the shrub and herb PFTs. We found that the site characteristics, particularly latitude for the shrub PFTs and air temperature for evergreen needleleaf tree, explained much of the spatial variability, providing a basis to improve V_{cmax25} parameterizations in TBMs at regional scales.

https://doi.org/10.5194/egusphere-2023-1167
Preprint. Discussion started: 19 July 2023

1 Introduction

Photosynthesis is an important ecosystem function that underlies tightly coupled carbon and water fluxes (Beer et al., 2010; Keenan and Williams, 2018). Spatially varying abiotic and biotic conditions including climate, vegetation, disturbance history, soil type, soil nutrient availability, and permafrost controls photosynthesis across the boreal biome through complex interactions (Loranty et al., 2016; Bergeron et al., 2007; Ueyama et al., 2015). This complexity greatly challenges accurate predictions of carbon and water fluxes over the vast boreal biome by terrestrial biosphere models (TBMs) (Fisher et al., 2018; Mcguire et al., 2016), such as the Canadian Land Surface Scheme Including biogeochemical Cycles (CLASSIC) (Curasi et al., 2023).

Eddy covariance observations of carbon dioxide (CO_2) and water fluxes provide valuable data for TBM refinement and development (Schwalm et al., 2010; Bonan et al., 2011). CLASSIC performance for CO_2 and water fluxes showed great variations across North America's boreal forests compared with eddy covariance observations (Qu et al., 2022). The model-observation discrepancies were due in part to varied errors in gross primary production (GPP), i.e., photosynthetic CO_2 uptake, and evapotranspiration (ET).

The "Farquhar" model and its variants are frequently used in TBMs including CLASSIC to simulate GPP and ET with coupled stomatal conductance–photosynthesis models (Farquhar et al., 1980; Rogers, 2014). The maximum rates of RuBisCO carboxylation, V_{cmax}, is one of the most important parameters in the "Farquhar" model. However, V_{cmax} parameterizations are generally oversimplified in TBMs and assume that V_{cmax} for plant functional types (PFTs) is constant in time and space. V_{cmax} is thus widely identified as a critical source of uncertainty in modelling GPP and ET (Collatz et al., 1991; Bonan et al., 2011). Estimates of V_{cmax} vary greatly among and within plant species (Yan et al., 2023). Foliar nutrients invested in photosynthetic proteins, particularly in the RuBisCO enzyme, determine V_{cmax} (Evans and Seemann, 1989). Through their influence on foliar nutrient concentrations, morphology, and nutrient use efficiency of photosynthesis (Musavi et al., 2016; Maire et al., 2015; Dong et al., 2020), environmental variables such as air temperature, solar radiation, and atmospheric humidity were found to exert strong controls on V_{cmax} (Ali et al., 2015; Yan et al., 2023). The boreal biome is characterized by short growing seasons, low rates of soil mineralization and limited nutrient availability, especially in the permafrost zone (Price et al., 2013). Plant phenology, closely associated with soil freeze-thaw and nutrient cycling (Rayment et al., 2002) and the seasonality of foliar ontogeny and chlorophyll content (Croft et al., 2017; Detto and Xu, 2020), may thus be important for V_{cmax} of boreal plant species.

Optimizing V_{cmax} in TBMs using eddy covariance observations for boreal forests has been the focus of several studies (He et al., 2014; Mo et al., 2008; Ueyama et al., 2016). However, those optimizations were performed only on a single tree PFT for one site, e.g., evergreen needleleaf tree. Boreal forests often have various shrub, herb, moss and lichen species that dominate the understory and ground cover, constituting non-negligible contributions to carbon and water fluxes (Gaumont-Guay et al., 2014). In this study, we optimized V_{cmax25} (V_{cmax} at 25 °C) in CLASSIC for boreal forests using GPP

https://doi.org/10.5194/egusphere-2023-1167
Preprint. Discussion started: 19 July 2023

and ET obtained from eddy covariance measurements made at eight black spruce (*Picea mariana*)-dominated, mature forest stands (>70 years old) (Qu et al., 2022). The optimizations were conducted for six (two tree, two shrub, and two herb) PFTs both at individual sites and across sites. Model performance using the optimized PFT-V_{cmax25} were compared with several corresponding stand-level estimates extracted from gridded global products. We compared the optimized PFT-V_{cmax25} to estimates derived from leaf-level gas exchange measurements reported in the literature. The PFT-V_{cmax25} variation and site characteristics underlying the variation was investigated using a random forest approach.

2 Methods

2.1 Model description

CLASSIC is the TBM of the Canadian Earth System Model (Melton et al., 2020). Leaf-level photosynthesis is simulated with the "Farquhar" photosynthesis model coupled to the "Leuning" stomatal conductance model (Collatz et al., 1991; Leuning, 1995; Farquhar et al., 1980). V_{cmax25} (μmol CO_2 m^{-2} s^{-1}) is prescribed for PFTs and is scaled to V_{cmax} (μmol CO_2 m^{-2} s^{-1}) based on canopy temperature and soil moisture:

$$V_{cmax} = \frac{S_{root}\, Q_{10}^{25℃}\, V_{cmax25}}{[1+\exp 0.3(T_c - T_{upper})][1+\exp 0.3(T_{lower} - T_c)]} \quad (1)$$

The scaling term uses the standard Q_{10} function at 25 ℃, soil moisture stress (S_{root}, unitless), canopy temperature (T_c, ℃), and PFT-specific temperature thresholds for photosynthesis (T_{lower} and T_{upper}, ℃) (Table S1). The soil moisture stress (S_{root}) on V_{cmax} is determined by the soil water content and the fraction of plant roots:

$$S_{root} = \sum_{i=1}^{g} r_i[1-(1-\emptyset_i)^2] \quad (2)$$

$$\emptyset_i = \max\left[0, \min\left(1, \frac{\theta_i - \theta_{i,wilt}}{\theta_{i,field} - \theta_{i,wilt}}\right)\right] \quad (3)$$

Specifically, it is estimated by the degree of soil wetness ($\emptyset_i$, unitless) and the fraction of roots (r_i) in each soil layer (i) over all soil layers (g). The degree of soil wetness ($\emptyset_i$) of the i^{th} soil layer is estimated by the volumetric soil moisture (θ_i, m^3 m^{-3}), wilting point ($\theta_{i,wilt}$, m^3 m^{-3}), and field capacity ($\theta_{i,field}$, m^3 m^{-3}).

The effects of photoperiod on the seasonality of V_{cmax25} are considered for high-latitude shrub and deciduous tree PFTs, i.e., "deciduous needleleaf tree" (DNT), "evergreen broadleaf shrub" (EBS), and "deciduous broadleaf shrub" (DBS), according to the ratio of day length on a given day (L_d, h) to the maximum day length over a year (L_{max}, h) (Bauerle et al., 2012; Meyer et al., 2021):

$$V_{cmax25}^{d} = V_{cmax25}\left(\frac{L_d}{L_{max}}\right)^2 \quad (4)$$

This study was conducted using the CLASSIC version 1.3 with twelve PFTs representing high latitudes (Meyer et al., 2021; Melton and Arora, 2016). We used two tree, i.e., "evergreen needleleaf tree" (ENT) and DNT, two shrub, i.e., EBS

https://doi.org/10.5194/egusphere-2023-1167
Preprint. Discussion started: 19 July 2023

and DBS, and two herb PFTs, i.e., "C3 grass" (C3G) and "sedge" (SDG), collectively representing the studied boreal forest stands (Qu et al., 2022).

2.2 Eddy covariance and supporting measurements

Our optimizations used a model benchmarking dataset comprising eddy covariance and supporting measurements made at eight mature boreal forest stands in North America (Table S2). The forest stands are dominated by black spruce in the overstory with canopy coverage ranging from 15 % to 90 %. Dominant understory vascular plants include dwarf shrubs, e.g., Labrador tea (*Rhododendron groenlandicum*), lingonberry (*Vaccinium vitis-idaea*), blueberry (*Vaccinium spp.*), and sedges (e.g., *Carex spp.*).

2.3 Bayesian optimization by tree-structured Parzen estimator

The tree-structured Parzen estimator (TPE), a Bayesian algorithm implemented in the Hyperopt Python package, was used for the optimization (Bergstra et al., 2015). TPE is an efficient algorithm to optimize hyperparameters (Bergstra et al., 2011; Nguyen et al., 2020). The cost function was defined by the normalized root mean square error ($RMSE_n$) of daily sum of GPP (g C m^{-2} day^{-1}) and ET (mm day^{-1}) between CLASSIC simulations and eddy covariance observations (Groenendijk et al., 2011):

$$RMSE_n = \frac{RMSE(\boldsymbol{GPP_{obs}}, \boldsymbol{GPP_{sim}})}{\overline{\boldsymbol{GPP_{obs}}}} + \frac{RMSE(\boldsymbol{ET_{obs}}, \boldsymbol{ET_{sim}})}{\overline{\boldsymbol{ET_{obs}}}} \quad (5)$$

The optimizations were limited to the growing seasons, delineated for each boreal forest stand and site-year using the daily GPP and a double-logistic function fitted to the daily GPP time series (Gonsamo et al., 2013; El-Amine et al., 2022). The prior uncertainties of V_{cmax25} were defined by a uniform space (Bergstra et al., 2015). The lower boundary was set to 10 μmol CO_2 m^{-2} s^{-1} for all PFTs to avoid optimizing unrealistically low V_{cmax25} (Rogers, 2014). The upper boundaries for the shrub and herb PFTs were set to 120 μmol CO_2 m^{-2} s^{-1} (EBS, DBS, and C3G) and 100 μmol CO_2 m^{-2} s^{-1} (SDG), i.e., 2 to 3 times higher than prior values in CLASSIC (Table S1) (Santaren et al., 2007; Kuppel et al., 2012). We set an upper boundary of 65 μmol CO_2 m^{-2} s^{-1} for the tree PFTs, i.e., ENT and DNT (Ueyama et al., 2018; Smith and Dukes, 2017). We conducted two types of optimizations: (1) at each forest stand ("single-site") and (2) pooled including all eight forest stands ("all-sites"). Every optimization at each stand ran for 500 iterations (Bergstra et al., 2011). For each iteration, a spin-up procedure was performed to equilibrate the model, defined by the total carbon pool varying less than 0.1 % compared to the last loop (Meyer et al., 2021). The simulation was conducted by running model one final loop starting from the equilibrium state. The optimization convergence was quantified with the 1 % quantile of the minimum cost function (Bergstra et al., 2011) (Fig. S1 and S2; Text S1).

https://doi.org/10.5194/egusphere-2023-1167
Preprint. Discussion started: 19 July 2023

2.4 Measured V_{cmax25} and corresponding stand-level estimates of GPP and ET

The optimized PFT-V_{cmax25} was compared to published estimates obtained from leaf-level gas exchange measurements (Smith et al., 2019; Kattge et al., 2009; Ali et al., 2015; Smith and Dukes, 2017; Bauerle et al., 2012). We collated the measurements made from the Arctic-boreal region or from other regions but for the dominant vascular species of the boreal forest stands (Table S3). To allow comparisons, we standardized measurements to 25 °C using an Arrhenius function (Smith et al., 2019; Kattge and Knorr, 2007). The CLASSIC GPP and ET using the optimized PFT-V_{cmax25} were compared with several corresponding stand-level estimates obtained from gridded global data products (Table 1; Text S2).

Table 1. Gridded global data products of gross primary production (GPP) and evapotranspiration (ET) used for comparison with stand-level simulations by CLASSIC using the optimized V_{cmax25}.

Data source	Fluxes	Approach	Temporal and spatial resolutions	Temporal coverage	Acronym
ORNL DAAC (Running and Zhao, 2021)	GPP, ET	MODIS MOD17A2HGF v061 (GPP) and MOD16A2GF v061 (ET).	8-day, 8 km	2000–2021	MODIS-OD
Li et al. (2021)	GPP, ET	Coupled process-based model driven by MODIS products.	Daily, 1 km	2001–2021	BESS
Li and Xiao (2019)	GPP	Statistical model driven by OCO-2 solar-induced chlorophyll fluorescence.	Monthly, 0.05°	2000–2018	GOSIF
Zhang et al. (2017)	GPP	Light use efficiency model driven by NCEP Reanalysis II climate and MODIS products.	Monthly, 0.05°	2000–2016	MODIS-Z
Liang et al. (2021)	GPP	Eddy covariance-derived light use efficiency model driven by AVHRR products.	Monthly, 0.05°	1982–2018	GLASS
Hobeichi et al. (2020)	ET	Data assimilation approach to conserve surface water and energy budget closure.	Monthly, 0.5°	2003–2009	CLASS

2.5 Statistical analyses

We derived the average and standard deviation of the posterior distributions to characterize the optimized PFT-V_{cmax25} (Santaren et al., 2007; Ueyama et al., 2016; Groenendijk et al., 2011). We used the root mean square deviation (RMSD) to evaluate CLASSIC performance using the prior and optimized PFT-V_{cmax25} (Kuppel et al., 2012). A random

https://doi.org/10.5194/egusphere-2023-1167
Preprint. Discussion started: 19 July 2023

forest approach was employed to investigate relationships between the "single-site" optimized PFT-V_{cmax25} and a suite of predictors including latitude, and metrics of growing season timing (i.e., start, end, and duration), and several environmental variables. Environmental variables included incoming shortwave radiation (SW, W m^{-2}), air temperature (TA, °C), total precipitation (P, mm), and vapor pressure deficit (VPD, hPa). We calculated the multi-year averages of growing-season averages (SW, TA, and VPD) and sums (P). In each random forest we employed 1000 decision trees using the scikit-learn Python package (Breiman, 2001). The importance of the predictors was estimated using the impurity-based feature importance (Strobl et al., 2007). Partial dependence plots were produced to illustrate the relationships (Goldstein et al., 2015; Baltzer et al., 2021).

3 Results and discussion

3.1 Model simulations using optimized PFT-V_{cmax25}

Model performance regarding GPP and ET improved at most forest stands (e.g., lower RMSD) using the "single-site" optimized PFT-V_{cmax25} (Fig. 1a and b). Exceptions include GPP at US-Uaf and ET at US-BZS and US-Prr. Similar improvements were achieved with the "all-sites" optimization (Table S4).

Compared with the corresponding stand-level estimates, RMSD of GPP using the "single-site" optimized PFT-V_{cmax25} was reduced among almost all estimates and sites (Fig. 1c). The reduction in RMSD averaged ($RMSD_a$) over the corresponding stand-level estimates was more notable at the sites with higher $RMSD_a$ using the prior PFT-V_{cmax25}. For ET, a notable reduction in $RMSD_a$ using the "single-site" optimized PFT-V_{cmax25} was found at two permafrost-free sites, CA-Qfo and CA-Obs, where $RMSD_a$ decreased by 42 % at each site (Fig. 1d). In contrast, $RMSD_a$ of ET using the "single-site" optimized PFT-V_{cmax25} was unchanged for the other sites. The "all-sites" optimized PFT-V_{cmax25} yielded similar results, reducing $RMSD_a$ by 59 % (GPP) and 12 % (ET), respectively, across all sites (Table S5).

https://doi.org/10.5194/egusphere-2023-1167
Preprint. Discussion started: 19 July 2023

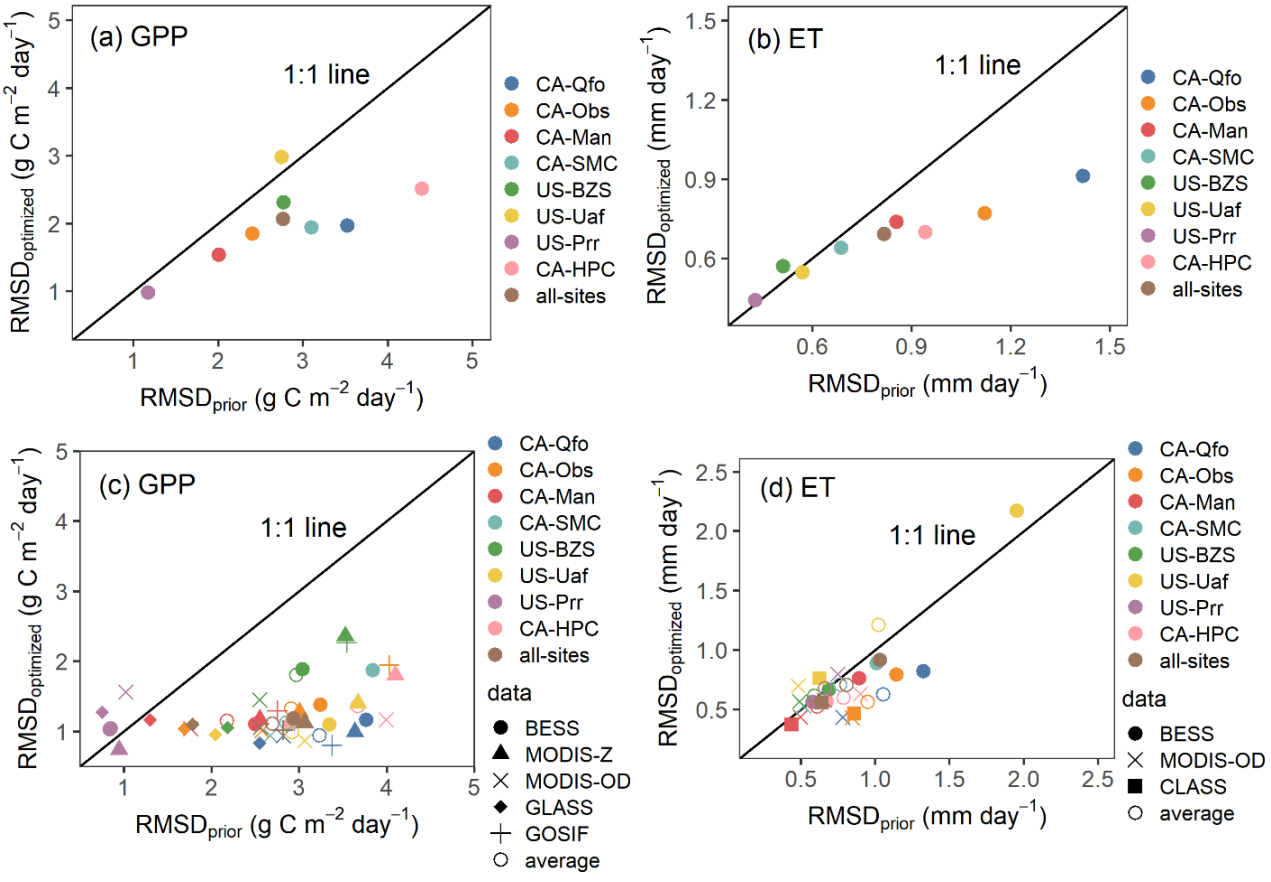

Figure 1. Root mean square deviation (RMSD) of CLASSIC gross primary production (GPP) and evapotranspiration (ET) using the prior and optimized plant functional type-V_{cmax25} ("single-site" and "all-sites") compared with eddy covariance observations (a, b) and corresponding stand-level estimates (c, d; Table 1). Site names refer to AmeriFlux ID and sites are ordered by latitude from south (CA-Qfo) to north (CA-HPC) (Table S2).

3.2 Optimized PFT-V_{cmax25}

The "all-sites" optimized PFT-V_{cmax25} showed large differences from the prior values except for DNT and DBS (Fig. 2a). The optimized V_{cmax25} was reduced by approximately 35 % for ENT and EBS and increased by 96 % and 32 % for SDG and C3G, respectively. Similarly, differences between the prior and "single-site" optimized PFT-V_{cmax25} were found. For example, a large variation in PFT-V_{cmax25} was found for shrub PFTs and SDG.

Black spruce is one of the dominant needleleaf evergreen tree species in North America's boreal forests and the most abundant tree species at all study sites (>90 %; Qu et al., 2022). The measured V_{cmax25} for black spruce ranged from 20 to 30 μmol CO_2 m^{-2} s^{-1} in the boreal biome (Fig. 2b; Table S3), comparable to our optimized V_{cmax25} for ENT ("single-site": 24–36 μmol CO_2 m^{-2} s^{-1}; "all-sites": 27 μmol CO_2 m^{-2} s^{-1}) except for US-BZS (Fig. 2a). The published estimates of measured

https://doi.org/10.5194/egusphere-2023-1167
Preprint. Discussion started: 19 July 2023

V_{cmax25} for shrub and herb PFTs were limited but varied widely among measurements (Fig. 2b). Consistent with our optimizations, the large variation in these estimates indicated great uncertainties of the V_{cmax25} for shrub and herb PFTs. The optimized V_{cmax25} for EBS and DBS at CA-Qfo and CA-Man (the permafrost-free forest stands) was relatively high but still comparable to the upper limits of measurements. The optimized V_{cmax25} for shrub PFTs and SDG at the forest stands in the permafrost zone fell in the ranges of measurements. The optimized V_{cmax25} for ENT, EBS, and DBS at US-Uaf was in good agreement with measurements made at this site (Ueyama et al., 2018).

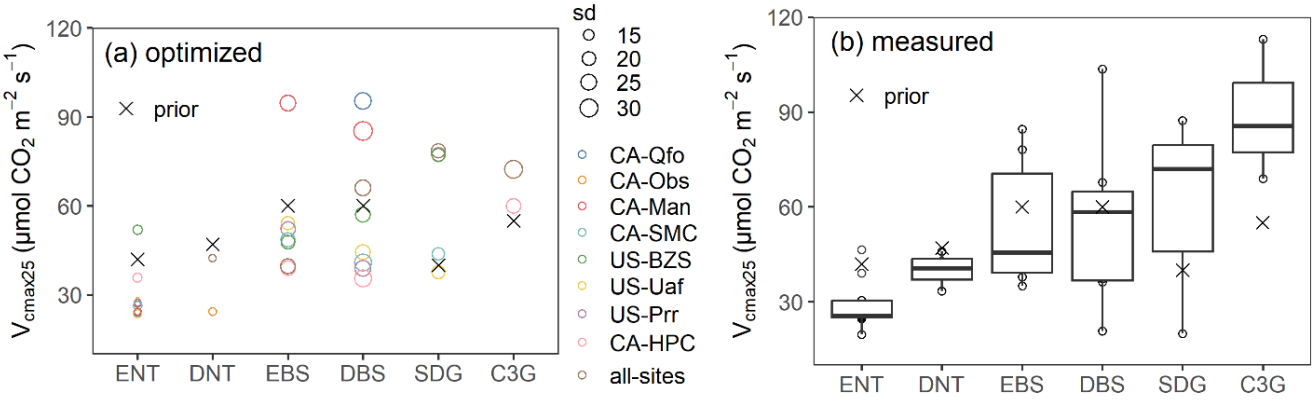

Figure 2. Plant functional type (PFT)-V_{cmax25} from (a) "single-site" and "all-sites" optimizations and (b) the reported estimates from leaf-level gas exchange measurements (Table S3) compared to the prior V_{cmax25} in CLASSIC. CLASSIC PFTs are "evergreen needleleaf tree" (ENT), "deciduous needleleaf tree" (DNT), "evergreen broadleaf shrub" (EBS), "deciduous broadleaf shrub" (DBS), "C3 grass" (C3G), and "sedge" (SDG). In panel (a), point sizes indicate the standard deviation (sd; μmol CO_2 m^{-2} s^{-1}) of PFT-V_{cmax25}. Site names refer to AmeriFlux ID and sites are ordered by latitude from south (CA-Qfo) to north (CA-HPC) (Table S2).

3.3 Variation in PFT-V_{cmax25} and links to site characteristics

Random forest regressions suggested that the variations in the optimized PFT-V_{cmax25} among the mature boreal forest stands were well explained by the selected predictors related to site characteristics (R^2 = 0.79 to 0.93, Table 2). A latitudinal gradient in V_{cmax25} for shrub PFTs indicated that shrubs in higher latitudes had lower V_{cmax25} (importance ≥ 0.3; Fig. S3). For ENT, TA had a strong influence on V_{cmax25} (importance = 0.35); lower TA was associated with lower V_{cmax25}. The findings for ENT are supported by measurements for black spruce made in the temperate biome which were higher than those made in the boreal biome (Table S3). For ENT and shrub PFTs, the start (SOS) or end of growing seasons (EOS) were important variables (importance > 0.2). Generally, the sites with early SOS or late EOS tended to have a high V_{cmax25}. SW was found to be influential for the V_{cmax25} of SDG (importance = 0.22); other predictors were relatively less important for this PFT.

Several global analyses of V_{cmax25} suggested a latitudinal gradient in V_{cmax25} with relatively high values for high-latitude PFTs (Ali et al., 2015; Kattge et al., 2009). However, measurements from the boreal biome were very limited in

https://doi.org/10.5194/egusphere-2023-1167
Preprint. Discussion started: 19 July 2023

these studies. To date, comprehensive measurement-based studies investigating the spatial variation in V_{cmax25} are lacking for boreal plant taxa and associated PFTs. Our findings suggest that differences in representation by dominant PFTs in mature boreal forest stands was important for explaining variation in V_{cmax25}. For example, ENT with low V_{cmax25} was dominant at the southern permafrost-free stands while shrub and herb PFTs with relatively high V_{cmax25} were more abundant at the northern forest stands in the permafrost zone.

Plant species richness, relative abundance, and composition is likely critical in understanding variations in PFT-V_{cmax25}. Shrub and herb PFTs has greater variations in the optimized V_{cmax25}, which may partly reflect the greater diversity of shrub and herb species compared to tree species in the boreal biome (Qu et al., 2022).

Table 2. The model accuracy of random forest regressions to predict plant functional type (PFT)-V_{cmax25} and relative importance of the selected predictors. Growing season metrics are the start (SOS, day of year), end (EOS, day of year), and duration (LOS, days). Latitude (LAT, °), incoming shortwave radiation (SW, W m^{-2}), air temperature (TA, °C), total precipitation (P, mm), and vapor pressure deficit (VPD, hPa). CLASSIC PFTs are "evergreen needleleaf tree" (ENT), "evergreen broadleaf shrub" (EBS), "deciduous broadleaf shrub" (DBS), and "sedge" (SDG). Bold fonts label the importance greater than 0.2.

PFT	R^2	Relative Importance							
		LAT	SOS	EOS	LOS	SW	TA	P	VPD
ENT	0.79	0.07	**0.21**	0.05	0.08	0.03	**0.35**	0.08	0.14
EBS	0.81	**0.33**	0.13	**0.22**	0.06	0.07	0.04	0.03	0.11
DBS	0.93	**0.30**	0.13	**0.21**	0.10	0.06	0.05	0.07	0.08
SDG	0.84	0.07	0.11	0.14	0.12	**0.22**	0.10	0.12	0.11

3.4 Implications

Our optimizations indicated that the overestimated V_{cmax25} for ENT as the prior value in CLASSIC might be a main cause for overestimating GPP and ET in boreal forests (Qu et al., 2022). Many TBMs including CLASSIC do not include explicit parametrizations for boreal ENT, according to a review of eleven TBMs that employed the "Farquhar" model (Rogers, 2014). Explicitly representing boreal ENT would thus be important to improve the performance of TBMs in the vast boreal biome. Our results further suggested that incorporating a V_{cmax25}-TA relationship could improve V_{cmax25} parametrizations for ENT (Wullschleger et al., 2014; Verheijen et al., 2013).

Due in part to the limited measurements for high-latitude plant species, shrub and herb PFTs parameterized for the boreal biome may largely depend on the estimates from non-boreal species (Rogers et al., 2017). Our optimizations identified great uncertainties in V_{cmax25} estimates for shrub and herbs PFTs, indicating this as a key challenge for accurate V_{cmax25} parameterizations for these PFTs in the boreal biome. This is particularly important for the permafrost zone given the important contributions of shrubs and herbs to the boreal forest functioning (Warren et al., 2018; Ikawa et al., 2015).

https://doi.org/10.5194/egusphere-2023-1167
Preprint. Discussion started: 19 July 2023

Allowing V_{cmax25} to vary with latitudes may provide an improved V_{cmax25} parameterizations for shrub PFTs. Sedges are parameterized in CLASSIC but are an under-represented PFT in many TBMs (Rogers, 2014). Sedges presented up to 40 % of plants at the study boreal forest stands in the permafrost zone (Qu et al., 2022). Our optimizations suggested that distinguishing SDG from the commonly used herb PFT, e.g., C3G, is important to parameterize herbs for the boreal biome.

3.5 Limitations

Our V_{cmax25} optimizations encounter several sources of uncertainty associated with the measurements in the model benchmarking dataset, the model representations of soils, permafrost, and plants, the model parametrizations for photosynthesis (e.g., V_{cmax25} seasonality) and evapotranspiration (e.g., stomatal conductance), and the optimization strategies employed.

Eddy covariance and supporting measurements include uncertainty from data collection and processing, e.g., the flux gap-filling (Soloway et al., 2017) and the partitioning of net ecosystem exchange into its component fluxes of GPP and ecosystem respiration (Lasslop et al., 2010; Reichstein et al., 2005). Additional uncertainty might be introduced through the ancillary measurements characterising soil and plants. For example, soil moisture generally varies across the boreal forest stands with soil drainage class (Wickland et al., 2010), microtopography, and permafrost, influencing soil nutrient availability and plant distribution (Chen et al., 2012; Helbig et al., 2016) and challenging model parameterizations (Rogers et al., 2021). The resulting overall uncertainty might be higher at the sites in the permafrost zone (Ueyama et al., 2016; Rogers et al., 2021).

The absent presentation of non-vascular plants in CLASSIC may constitute an important limitation and a source of uncertainty. Non-vascular plants including mosses and lichens are an important component of boreal forest functioning (Turetsky et al., 2012). For example, mosses at CA-Obs were reported to account for approximately 85 % of understory GPP (Gaumont-Guay et al., 2014) and 10–50 % of stand-level GPP (Goulden and Crill, 1997; Swanson and Flanagan, 2001). Various mosses (e.g., *Sphagnum* and feather moss) accounted for 27 % to 90 % of the ground cover among the study sites (Qu et al., 2022) and their functional properties in photosynthesis and evapotranspiration are distinct from vascular plants (Heijmans et al., 2004; Zha and Zhuang, 2021; Shi et al., 2021).

CLASSIC is a process-based TBM with sophisticated model structures and associated parameters to represent the interactions of terrestrial ecosystems with the atmosphere through the exchanges of energy and matter (Melton et al., 2020). For example, the simulated canopy properties, e.g., within-canopy profiles of photosynthesis (Bonan et al., 2012) and canopy conductance (Santaren et al., 2007), and the modelled permafrost dynamics in the permafrost zone (Schädel et al., 2018) may provide critical controls for simulating GPP and ET in the boreal biome. Uncertainty may also come from V_{cmax25} seasonality (Jensen et al., 2019). The day-length based V_{cmax25} seasonality was employed in CLASSIC for the PFTs known to exhibit pronounced V_{cmax25} seasonality, that have similarly been implemented in other TBMs, e.g., Community Land Model (Bauerle et al., 2012; Alton, 2017; Oberbauer et al., 2013). The high Pearson correlation coefficients suggested that the seasonal

https://doi.org/10.5194/egusphere-2023-1167
Preprint. Discussion started: 19 July 2023

variations in GPP and ET were well simulated by the assumption of V_{cmax25} seasonality in CLASSIC (Table S4). However, the day-length based seasonality may be oversimplified because measurements suggested that other environmental variables, e.g., air temperature and solar radiation, were also important for V_{cmax25} seasonality (Jensen et al., 2019; Ali et al., 2015).

Our cost function evaluated stand-level GPP and ET fluxes together. Results indicated that GPP was more sensitive to V_{cmax25} than ET (higher coefficients of variation determined from the ratio of standard deviation to mean, Table S4), which may partly explain the limited performance improvement for ET through V_{cmax25} optimizations at some of studied sites, especially in the permafrost zone (Fig. 1b). In addition, evaporation from ground cover may account for a large percentage of stand-level ET in the open boreal forest stands in the permafrost zone (Heijmans et al., 2004). The influence of V_{cmax25} on stand-level ET would thus be small through the coupled photosynthesis and stomatal conductance models in those regions.

We used two strategies to optimize the model: "single-site" and "all-sites" optimizations. Although both strategies provided consistent improvement in GPP and ET simulations, the optimized PFT-V_{cmax25} were different. The "all-sites" optimization provided a set of PFT-V_{cmax25} which was applicable for all sites, but uncertainty might result from small sample sizes for some PFTs, e.g., DNT (Fig. 2a). In contrast, uncertainty might be introduced from the "single-site" optimizations if parameterizing the model by simply using the averages of the "single-site" optimized PFT-V_{cmax25}. For example, the optimized V_{cmax25} for ENT at US-BZS was much higher than that at other sites or from the "all-sites" optimization. The "single-site" optimizations were, however, valuable in providing opportunities to understand spatial variability of PFT-V_{cmax25} and the influence of boreal environments.

4 Conclusions

With the "Farquhar" model implemented in CLASSIC, we performed Bayesian optimizations for PFT-V_{cmax25} at eight mature boreal forest stands using GPP and ET obtained from eddy covariance measurements. Comparisons of the model simulations using the optimized parameters with the corresponding stand-level estimates showed that the optimized PFT-V_{cmax25} substantially reduced model-data RMSD for GPP at almost all sites and ET at two permafrost-free sites, indicating the importance of improving V_{cmax25} parameterizations for boreal PFTs. We found that shrub and herb PFTs had larger spatial variability of V_{cmax25} than ENT. The spatial variability of PFT-V_{cmax25} was well linked to the site characteristics in latitude, TA, SW, and the start and end of growing seasons. Our study presented an important step for improved PFT-V_{cmax25} parameterizations for North America boreal forests in TBMs.

Code availability

The current version of model is available from the project website: https://gitlab.com/cccma/classic under the Open Government License – Canada and the GNU General Public License version 2. The version of the model (CLASSIC v.1.3)

https://doi.org/10.5194/egusphere-2023-1167
Preprint. Discussion started: 19 July 2023

used in this study, as well as the input data and scripts to perform the optimizations and to produce the plots presented in this paper, is archived on Zenodo (https://doi.org/10.5281/zenodo.8136578) (Qu et al., 2023).

Data availability

The model benchmarking dataset used in this study is available on Zenodo: https://doi.org/10.5281/zenodo.7266010 (Qu et al., 2022).

Author contribution

Bo Qu, Alexandre Roy, Joe R. Melton, and Oliver Sonnentag conceived this study and designed the research methodology. Bo Qu performed the optimizations and analyzed the results with inputs from all co-authors. Bo Qu prepared the manuscript with contributions from all co-authors.

Competing interests

The authors declare that they have no conflict of interest.

Acknowledgments

Bo Qu acknowledges funding from the China Scholarship Council and Centre d'Études Nordiques. Jennifer L. Baltzer acknowledges funding through the CFREF Global Water Futures – Northern Water Futures project and Canada Research Chairs Program. Youngryel Ryu was supported by the National Research Foundation of Korea (NRF-2021M1A5A1065681). Matteo Detto was supported by the Carbon Mitigation Initiative at Princeton University and NSF grant 2017804. Oliver Sonnentag acknowledges funding through the Canada Research Chairs, Canada Foundation for Innovation Leaders Opportunity Fund, and Natural Sciences and Engineering Research Council Discovery Grant programs. We thank the CLASSIC team for providing support. We thank the Compute Canada for computing resources.

References

Ali, A. A., Xu, C., Rogers, A., McDowell, N. G., Medlyn, B. E., Fisher, R. A., Wullschleger, S. D., Reich, P. B., Vrugt, J. A., and Bauerle, W. L.: Global-scale environmental control of plant photosynthetic capacity, Ecol. Appl., 25, 2349-2365, https://doi.org/10.1890/14-2111.1, 2015.

https://doi.org/10.5194/egusphere-2023-1167
Preprint. Discussion started: 19 July 2023

Alton, P. B.: Retrieval of seasonal Rubisco-limited photosynthetic capacity at global FLUXNET sites from hyperspectral satellite remote sensing: Impact on carbon modelling, Agr. Forest Meteorol., 232, 74-88, https://doi.org/10.1016/j.agrformet.2016.08.001, 2017.

Baltzer, J. L., Day, N. J., Walker, X. J., Greene, D., Mack, M. C., Alexander, H. D., Arseneault, D., Barnes, J., Bergeron, Y., and Boucher, Y.: Increasing fire and the decline of fire adapted black spruce in the boreal forest, PNAS, 118, e2024872118, https://doi.org/10.1073/pnas.2024872118, 2021.

Bauerle, W. L., Oren, R., Way, D. A., Qian, S. S., Stoy, P. C., Thornton, P. E., Bowden, J. D., Hoffman, F. M., and Reynolds, R. F.: Photoperiodic regulation of the seasonal pattern of photosynthetic capacity and the implications for carbon cycling, PNAS, 109, 8612-8617, https://doi.org/10.1073/pnas.1119131109, 2012.

Beer, C., Reichstein, M., Tomelleri, E., Ciais, P., Jung, M., Carvalhais, N., Rödenbeck, C., Arain, M. A., Baldocchi, D., and Bonan, G. B.: Terrestrial gross carbon dioxide uptake: global distribution and covariation with climate, Science, 329, 834-838, https://doi.org/10.1126/science.1184984, 2010.

Bergeron, O., Margolis, H. A., Black, T. A., Coursolle, C., Dunn, A. L., Barr, A. G., and Wofsy, S. C.: Comparison of carbon dioxide fluxes over three boreal black spruce forests in Canada, Glob. Change Biol., 13, 89-107, https://doi.org/10.1111/j.1365-2486.2006.01281.x, 2007.

Bergstra, J., Komer, B., Eliasmith, C., Yamins, D., and Cox, D. D.: Hyperopt: a python library for model selection and hyperparameter optimization, Comput. Sci. Discov., 8, 014008, https://doi.org/10.1088/1749-4699/8/1/014008, 2015.

Bergstra, J., Bardenet, R., Bengio, Y., and Kégl, B.: Algorithms for hyper-parameter optimization, in: Advances in Neural Information Processing Systems, Curran Associates, Inc., ISBN 9781618395993, 2011.

Bonan, G. B., Lawrence, P. J., Oleson, K. W., Levis, S., Jung, M., Reichstein, M., Lawrence, D. M., and Swenson, S. C.: Improving canopy processes in the Community Land Model version 4 (CLM4) using global flux fields empirically inferred from FLUXNET data, J. Geophys. Res.-Biogeo., 116, G02014, https://doi.org/10.1029/2010JG001593, 2011.

Bonan, G. B., Oleson, K. W., Fisher, R. A., Lasslop, G., and Reichstein, M.: Reconciling leaf physiological traits and canopy flux data: Use of the TRY and FLUXNET databases in the Community Land Model version 4, J. Geophys. Res.-Biogeo., 117, G02026, https://doi.org/10.1029/2011JG001913, 2012.

Breiman, L.: Random forests, Mach. Learn., 45, 5-32, https://doi.org/10.1023/A:1010933404324, 2001.

Chen, B., Coops, N. C., Fu, D., Margolis, H. A., Amiro, B. D., Black, T. A., Arain, M. A., Barr, A. G., Bourque, C. P.-A., and Flanagan, L. B.: Characterizing spatial representativeness of flux tower eddy-covariance measurements across the Canadian Carbon Program Network using remote sensing and footprint analysis, Remote Sens. Environ., 124, 742-755, https://doi.org/10.1016/j.rse.2012.06.007, 2012.

Collatz, G. J., Ball, J. T., Grivet, C., and Berry, J. A.: Physiological and environmental regulation of stomatal conductance, photosynthesis and transpiration: a model that includes a laminar boundary layer, Agr. Forest Meteorol., 54, 107-136, https://doi.org/10.1016/0168-1923(91)90002-8, 1991.

https://doi.org/10.5194/egusphere-2023-1167
Preprint. Discussion started: 19 July 2023

Croft, H., Chen, J. M., Luo, X., Bartlett, P., Chen, B., and Staebler, R. M.: Leaf chlorophyll content as a proxy for leaf photosynthetic capacity, Glob. Change Biol., 23, 3513-3524, https://doi.org/10.1111/gcb.13599, 2017.

Curasi, S. R., Melton, J. R., Humphreys, E. R., Wang, L., Seiler, C., Cannon, A. J., Chan, E., and Qu, B.: Evaluating the Performance of the Canadian Land Surface Scheme Including Biogeochemical Cycles (CLASSIC) Tailored to the Pan-Canadian Domain, J. Adv. Model. Earth Sy., 15, e2022MS003480, https://doi.org/10.1029/2022MS003480, 2023.

Detto, M. and Xu, X.: Optimal leaf life strategies determine Vc,max dynamic during ontogeny, New Phytol., 228, 361-375, https://doi.org/10.1111/nph.16712, 2020.

Dong, N., Prentice, I. C., Wright, I. J., Evans, B. J., Togashi, H. F., Caddy-Retalic, S., McInerney, F. A., Sparrow, B., Leitch, E., and Lowe, A. J.: Components of leaf-trait variation along environmental gradients, New Phytol., 228, 82-94, https://doi.org/10.1111/nph.16558, 2020.

El-Amine, M., Roy, A., Koebsch, F., Baltzer, J. L., Barr, A., Black, A., Ikawa, H., Iwata, H., Kobayashi, H., and Ueyama, M.: What explains the year-to-year variation in growing season timing of boreal black spruce forests?, Agr. Forest Meteorol., 324, 109113, https://doi.org/10.1016/j.agrformet.2022.109113, 2022.

Evans, J. R. and Seemann, J. R.: The allocation of protein nitrogen in the photosynthetic apparatus: costs, consequences, and control, Photosynthesis, 8, 183-205, 1989.

Farquhar, G. D., von Caemmerer, S. v., and Berry, J. A.: A biochemical model of photosynthetic CO2 assimilation in leaves of C3 species, Planta, 149, 78-90, https://doi.org/10.1007/BF00386231, 1980.

Fisher, J. B., Hayes, D. J., Schwalm, C. R., Huntzinger, D. N., Stofferahn, E., Schaefer, K., Luo, Y., Wullschleger, S. D., Goetz, S., and Miller, C. E.: Missing pieces to modeling the Arctic-Boreal puzzle, Environ. Res. Lett., 13, 020202, https://doi.org/10.1088/1748-9326/aa9d9a, 2018.

Gaumont-Guay, D., Black, T., Barr, A., Griffis, T., Jassal, R., Krishnan, P., Grant, N., and Nesic, Z.: Eight years of forest-floor CO2 exchange in a boreal black spruce forest: Spatial integration and long-term temporal trends, Agr. Forest Meteorol., 184, 25-35, https://doi.org/10.1016/j.agrformet.2013.08.010, 2014.

Goldstein, A., Kapelner, A., Bleich, J., and Pitkin, E.: Peeking inside the black box: Visualizing statistical learning with plots of individual conditional expectation, J. Comput. Graph. Stat., 24, 44-65, https://doi.org/10.1080/10618600.2014.907095, 2015.

Gonsamo, A., Chen, J. M., and D'Odorico, P.: Deriving land surface phenology indicators from CO2 eddy covariance measurements, Ecol. Indic., 29, 203-207, https://doi.org/10.1016/j.ecolind.2012.12.026, 2013.

Goulden, M. and Crill, P.: Automated measurements of CO2 exchange at the moss surface of a black spruce forest, Tree Physiol., 17, 537-542, https://doi.org/10.1093/treephys/17.8-9.537, 1997.

Groenendijk, M., Dolman, A., Van Der Molen, M., Leuning, R., Arneth, A., Delpierre, N., Gash, J., Lindroth, A., Richardson, A., and Verbeeck, H.: Assessing parameter variability in a photosynthesis model within and between plant functional types using global Fluxnet eddy covariance data, Agr. Forest Meteorol., 151, 22-38, https://doi.org/10.1016/j.agrformet.2010.08.013, 2011.

https://doi.org/10.5194/egusphere-2023-1167
Preprint. Discussion started: 19 July 2023

He, L., Chen, J. M., Liu, J., Mo, G., Bélair, S., Zheng, T., Wang, R., Chen, B., Croft, H., and Arain, M. A.: Optimization of water uptake and photosynthetic parameters in an ecosystem model using tower flux data, Ecol. Model., 294, 94-104, https://doi.org/10.1016/j.ecolmodel.2014.09.019, 2014.

Heijmans, M. M., Arp, W. J., and Chapin III, F. S.: Controls on moss evaporation in a boreal black spruce forest, Global Biogeochem. Cy., 18, GB2004, https://doi.org/10.1029/2003GB002128, 2004.

Helbig, M., Wischnewski, K., Kljun, N., Chasmer, L. E., Quinton, W. L., Detto, M., and Sonnentag, O.: Regional atmospheric cooling and wetting effect of permafrost thaw-induced boreal forest loss, Glob. Change Biol., 22, 4048-4066, https://doi.org/10.1111/gcb.13348, 2016.

Hobeichi, S., Abramowitz, G., and Evans, J.: Conserving Land–Atmosphere Synthesis Suite (CLASS), J. Climate, 33, 1821-1844, https://doi.org/10.1175/JCLI-D-19-0036.1, 2020.

Ikawa, H., Nakai, T., Busey, R. C., Kim, Y., Kobayashi, H., Nagai, S., Ueyama, M., Saito, K., Nagano, H., and Suzuki, R.: Understory CO2, sensible heat, and latent heat fluxes in a black spruce forest in interior Alaska, Agr. Forest Meteorol., 214, 80-90, https://doi.org/10.1016/j.agrformet.2015.08.247, 2015.

Jensen, A. M., Warren, J. M., King, A. W., Ricciuto, D. M., Hanson, P. J., and Wullschleger, S. D.: Simulated projections of boreal forest peatland ecosystem productivity are sensitive to observed seasonality in leaf physiology, Tree Physiol., 39, 556-572, https://doi.org/10.1093/treephys/tpy140, 2019.

Kattge, J. and Knorr, W.: Temperature acclimation in a biochemical model of photosynthesis: a reanalysis of data from 36 species, Plant Cell Environ., 30, 1176-1190, https://doi.org/10.1111/j.1365-3040.2007.01690.x, 2007.

Kattge, J., Knorr, W., Raddatz, T., and Wirth, C.: Quantifying photosynthetic capacity and its relationship to leaf nitrogen content for global-scale terrestrial biosphere models, Glob. Change Biol., 15, 976-991, https://doi.org/10.1111/j.1365-2486.2008.01744.x, 2009.

Keenan, T. and Williams, C.: The terrestrial carbon sink, Annu. Rev. Env. Resour., 43, 219-243, https://doi.org/10.1146/annurev-environ-102017-030204, 2018.

Kuppel, S., Peylin, P., Chevallier, F., Bacour, C., Maignan, F., and Richardson, A.: Constraining a global ecosystem model with multi-site eddy-covariance data, Biogeosciences, 9, 3757-3776, https://doi.org/10.5194/bg-9-3757-2012, 2012.

Lasslop, G., Reichstein, M., Papale, D., Richardson, A. D., Arneth, A., Barr, A., Stoy, P., and Wohlfahrt, G.: Separation of net ecosystem exchange into assimilation and respiration using a light response curve approach: critical issues and global evaluation, Glob. Change Biol., 16, 187-208, https://doi.org/10.1111/j.1365-2486.2009.02041.x, 2010.

Leuning, R.: A critical appraisal of a combined stomatal-photosynthesis model for C3 plants, Plant Cell Environ., 18, 339-355, https://doi.org/10.1111/j.1365-3040.1995.tb00370.x, 1995.

Li, B., Ryu, Y., Jiang, C., Dechant, B., Liu, J., and Yan, Y.: BESS v2.0: A Satellite-driven and Coupled-process Model for Quantifying Global Land-atmosphere Radiation, Energy and CO2 Fluxes since 1982, AGU Fall Meeting 2021, New Orleans, LA, 13-17 December 2021, B15D-1463, 2021.

https://doi.org/10.5194/egusphere-2023-1167
Preprint. Discussion started: 19 July 2023

Li, X. and Xiao, J.: A global, 0.05-degree product of solar-induced chlorophyll fluorescence derived from OCO-2, MODIS, and reanalysis data, Remote Sens., 11, 517, https://doi.org/10.3390/rs11050517, 2019.

Liang, S., Cheng, J., Jia, K., Jiang, B., Liu, Q., Xiao, Z., Yao, Y., Yuan, W., Zhang, X., and Zhao, X.: The global land surface satellite (GLASS) product suite, B. Am. Meteorol. Soc., 102, E323-E337, https://doi.org/10.1175/BAMS-D-18-0341.1, 2021.

Loranty, M. M., Lieberman-Cribbin, W., Berner, L. T., Natali, S. M., Goetz, S. J., Alexander, H. D., and Kholodov, A. L.: Spatial variation in vegetation productivity trends, fire disturbance, and soil carbon across arctic-boreal permafrost ecosystems, Environ. Res. Lett., 11, 095008, https://doi.org/10.1088/1748-9326/11/9/095008, 2016.

Maire, V., Wright, I. J., Prentice, I. C., Batjes, N. H., Bhaskar, R., van Bodegom, P. M., Cornwell, W. K., Ellsworth, D., Niinemets, Ü., and Ordonez, A.: Global effects of soil and climate on leaf photosynthetic traits and rates, Global Ecol. Biogeogr., 24, 706-717, https://doi.org/10.1111/geb.12296, 2015.

McGuire, A. D., Koven, C., Lawrence, D. M., Clein, J. S., Xia, J., Beer, C., Burke, E., Chen, G., Chen, X., and Delire, C.: Variability in the sensitivity among model simulations of permafrost and carbon dynamics in the permafrost region between 1960 and 2009, Global Biogeochem. Cy., 30, 1015-1037, https://doi.org/10.1002/2016GB005405, 2016.

Melton, J. R. and Arora, V. K.: Competition between plant functional types in the Canadian Terrestrial Ecosystem Model (CTEM) v.2.0, Geosci. Model Dev., 9, 323-361, https://doi.org/10.5194/gmd-9-323-2016, 2016.

Melton, J. R., Arora, V. K., Wisernig-Cojoc, E., Seiler, C., Fortier, M., Chan, E., and Teckentrup, L.: CLASSIC v1.0: the open-source community successor to the Canadian Land Surface Scheme (CLASS) and the Canadian Terrestrial Ecosystem Model (CTEM)–Part 1: Model framework and site-level performance, Geosci. Model Dev., 13, 2825-2850, https://doi.org/10.5194/gmd-13-2825-2020, 2020.

Meyer, G., Humphreys, E. R., Melton, J. R., Cannon, A. J., and Lafleur, P. M.: Simulating shrubs and their energy and carbon dioxide fluxes in Canada's Low Arctic with the Canadian Land Surface Scheme Including Biogeochemical Cycles (CLASSIC), Biogeosciences, 18, 3263-3283, https://doi.org/10.5194/bg-18-3263-2021, 2021.

Mo, X., Chen, J. M., Ju, W., and Black, T. A.: Optimization of ecosystem model parameters through assimilating eddy covariance flux data with an ensemble Kalman filter, Ecol. Model., 217, 157-173, https://doi.org/10.1016/j.ecolmodel.2008.06.021, 2008.

Musavi, T., Migliavacca, M., van de Weg, M. J., Kattge, J., Wohlfahrt, G., van Bodegom, P. M., Reichstein, M., Bahn, M., Carrara, A., and Domingues, T. F.: Potential and limitations of inferring ecosystem photosynthetic capacity from leaf functional traits, Ecol. Evol., 6, 7352-7366, https://doi.org/10.1002/ece3.2479, 2016.

Nguyen, H.-P., Liu, J., and Zio, E.: A long-term prediction approach based on long short-term memory neural networks with automatic parameter optimization by Tree-structured Parzen Estimator and applied to time-series data of NPP steam generators, Appl. Soft Comput., 89, 106116, https://doi.org/10.1016/j.asoc.2020.106116, 2020.

https://doi.org/10.5194/egusphere-2023-1167
Preprint. Discussion started: 19 July 2023

Oberbauer, S., Elmendorf, S., Troxler, T., Hollister, R., Rocha, A., Bret-Harte, M., Dawes, M., Fosaa, A., Henry, G., and Høye, T.: Phenological response of tundra plants to background climate variation tested using the International Tundra Experiment, Philos. T. Roy. Soc. B, 368, 20120481, https://doi.org/10.1098/rstb.2012.0481, 2013.

Price, D. T., Alfaro, R., Brown, K., Flannigan, M., Fleming, R. A., Hogg, E., Girardin, M., Lakusta, T., Johnston, M., and McKenney, D.: Anticipating the consequences of climate change for Canada's boreal forest ecosystems, Environ. Rev., 21, 322-365, https://doi.org/10.1139/er-2013-0042, 2013.

Qu, B., Roy, A., Melton, J. R., Baltzer, J. L., Ryu, Y., Detto, M., and Sonnentag, O.: PFT-Vcmax25 optimization in CLASSIC (v.1.3), Zenodo [code], https://doi.org/10.5281/zenodo.8136578, 2023.

Qu, B., Sonnentag, O., Roy, A., Melton, J. R., Black, T. A., Amiro, B., Euskirchen, E. S., Ueyama, M., Kobayashi, H., Schulze, C., Gosselin, G. H., and Cannon, A. J.: A boreal forest model benchmarking dataset for North America: a case study with the Canadian Land Surface Scheme including Biogeochemical Cycles (CLASSIC), Zenodo [data set], https://doi.org/10.5281/zenodo.7266010, 2022.

Rayment, M., Loustau, D., and Jarvis, P.: Photosynthesis and respiration of black spruce at three organizational scales: shoot, branch and canopy, Tree Physiol., 22, 219-229, https://doi.org/10.1093/treephys/22.4.219, 2002.

Reichstein, M., Falge, E., Baldocchi, D., Papale, D., Aubinet, M., Berbigier, P., Bernhofer, C., Buchmann, N., Gilmanov, T., and Granier, A.: On the separation of net ecosystem exchange into assimilation and ecosystem respiration: review and improved algorithm, Glob. Change Biol., 11, 1424-1439, https://doi.org/10.1111/j.1365-2486.2005.001002.x, 2005.

Rogers, A.: The use and misuse of Vc,max in Earth System Models, Photosynth. Res., 119, 15-29, https://doi.org/10.1007/s11120-013-9818-1, 2014.

Rogers, A., Serbin, S. P., Ely, K. S., Sloan, V. L., and Wullschleger, S. D.: Terrestrial biosphere models underestimate photosynthetic capacity and CO2 assimilation in the Arctic, New Phytol., 216, 1090-1103, https://doi.org/10.1111/nph.14740, 2017.

Rogers, A., Serbin, S. P., and Way, D. A.: Reducing model uncertainty of climate change impacts on high latitude carbon assimilation, Glob. Change Biol., 28, 1222– 1247, https://doi.org/10.1111/gcb.15958, 2021.

Running, S. and Zhao, M.: MOD17A2HGF MODIS/Terra Gross Primary Productivity Gap-Filled 8-Day L4 Global 500 m SIN Grid V061, NASA EOSDIS Land Processes DAAC [data set], https://doi.org/10.5067/MODIS/MOD17A2HGF.061, 2021.

Santaren, D., Peylin, P., Viovy, N., and Ciais, P.: Optimizing a process-based ecosystem model with eddy-covariance flux measurements: A pine forest in southern France, Global Biogeochem. Cy., 21, GB2013, https://doi.org/10.1029/2006GB002834, 2007.

Schädel, C., Koven, C. D., Lawrence, D. M., Celis, G., Garnello, A. J., Hutchings, J., Mauritz, M., Natali, S. M., Pegoraro, E., and Rodenhizer, H.: Divergent patterns of experimental and model-derived permafrost ecosystem carbon dynamics in response to Arctic warming, Environ. Res. Lett., 13, 105002, https://doi.org/10.1088/1748-9326/aae0ff, 2018.

https://doi.org/10.5194/egusphere-2023-1167
Preprint. Discussion started: 19 July 2023

Schwalm, C. R., Williams, C. A., Schaefer, K., Anderson, R., Arain, M. A., Baker, I., Barr, A., Black, T. A., Chen, G., and Chen, J. M.: A model-data intercomparison of CO2 exchange across North America: Results from the North American Carbon Program site synthesis, J. Geophys. Res.-Biogeo., 115, G00H05, https://doi.org/10.1029/2009JG001229, 2010.

Shi, X., Ricciuto, D. M., Thornton, P. E., Xu, X., Yuan, F., Norby, R. J., Walker, A. P., Warren, J. M., Mao, J., and Hanson, P. J.: Extending a land-surface model with Sphagnum moss to simulate responses of a northern temperate bog to whole ecosystem warming and elevated CO2, Biogeosciences, 18, 467-486, https://doi.org/10.5194/bg-18-467-2021, 2021.

Smith, N. G. and Dukes, J. S.: LCE: Leaf carbon exchange data set for tropical, temperate, and boreal species of North and Central America, Ecology, 98, 2978, https://doi.org/10.1002/ecy.1992, 2017.

Smith, N. G., Keenan, T. F., Colin Prentice, I., Wang, H., Wright, I. J., Niinemets, Ü., Crous, K. Y., Domingues, T. F., Guerrieri, R., and Yoko Ishida, F.: Global photosynthetic capacity is optimized to the environment, Ecol. Lett., 22, 506-517, https://doi.org/10.1111/ele.13210, 2019.

Soloway, A. D., Amiro, B. D., Dunn, A. L., and Wofsy, S. C.: Carbon neutral or a sink? Uncertainty caused by gap-filling long-term flux measurements for an old-growth boreal black spruce forest, Agr. Forest Meteorol., 233, 110-121, https://doi.org/10.1016/j.agrformet.2016.11.005, 2017.

Strobl, C., Boulesteix, A.-L., Zeileis, A., and Hothorn, T.: Bias in random forest variable importance measures: Illustrations, sources and a solution, BMC bioinformatics, 8, 25, https://doi.org/10.1186/1471-2105-8-25, 2007.

Swanson, R. V. and Flanagan, L. B.: Environmental regulation of carbon dioxide exchange at the forest floor in a boreal black spruce ecosystem, Agr. Forest Meteorol., 108, 165-181, https://doi.org/10.1016/S0168-1923(01)00243-X, 2001.

Turetsky, M. R., Bond-Lamberty, B., Euskirchen, E., Talbot, J., Frolking, S., McGuire, A. D., and Tuittila, E. S.: The resilience and functional role of moss in boreal and arctic ecosystems, New Phytol., 196, 49-67, https://doi.org/10.1111/j.1469-8137.2012.04254.x, 2012.

Ueyama, M., Kudo, S., Iwama, C., Nagano, H., Kobayashi, H., Harazono, Y., and Yoshikawa, K.: Does summer warming reduce black spruce productivity in interior Alaska?, J. Forest Res.-Jpn, 20, 52-59, https://doi.org/10.1007/s10310-014-0448-z, 2015.

Ueyama, M., Tahara, N., Iwata, H., Euskirchen, E. S., Ikawa, H., Kobayashi, H., Nagano, H., Nakai, T., and Harazono, Y.: Optimization of a biochemical model with eddy covariance measurements in black spruce forests of Alaska for estimating CO2 fertilization effects, Agr. Forest Meteorol., 222, 98-111, https://doi.org/10.1016/j.agrformet.2016.03.007, 2016.

Ueyama, M., Tahara, N., Nagano, H., Makita, N., Iwata, H., and Harazono, Y.: Leaf-and ecosystem-scale photosynthetic parameters for the overstory and understory of boreal forests in interior Alaska, J. Agric. Meteorol., 74, 79-86, https://doi.org/10.2480/agrmet.D-17-00031, 2018.

Verheijen, L., Brovkin, V., Aerts, R., Bönisch, G., Cornelissen, J., Kattge, J., Reich, P. B., Wright, I. J., and Van Bodegom, P.: Impacts of trait variation through observed trait–climate relationships on performance of an Earth system model: a conceptual analysis, Biogeosciences, 10, 5497-5515, https://doi.org/10.5194/bg-10-5497-2013, 2013.

https://doi.org/10.5194/egusphere-2023-1167
Preprint. Discussion started: 19 July 2023

Warren, R. K., Pappas, C., Helbig, M., Chasmer, L. E., Berg, A. A., Baltzer, J. L., Quinton, W. L., and Sonnentag, O.: Minor contribution of overstorey transpiration to landscape evapotranspiration in boreal permafrost peatlands, Ecohydrology, 11, e1975, https://doi.org/10.1002/eco.1975, 2018.

Wickland, K. P., Neff, J. C., and Harden, J. W.: The role of soil drainage class in carbon dioxide exchange and decomposition in boreal black spruce (Picea mariana) forest stands, Can. J. Forest Res., 40, 2123-2134, https://doi.org/10.1139/X10-163, 2010.

Wullschleger, S. D., Epstein, H. E., Box, E. O., Euskirchen, E. S., Goswami, S., Iversen, C. M., Kattge, J., Norby, R. J., van Bodegom, P. M., and Xu, X.: Plant functional types in Earth system models: past experiences and future directions for application of dynamic vegetation models in high-latitude ecosystems, Ann. Bot.-London, 114, 1-16, https://doi.org/10.1093/aob/mcu077, 2014.

Yan, Z., Sardans, J., Peñuelas, J., Detto, M., Smith, N. G., Wang, H., Guo, L., Hughes, A. C., Guo, Z., and Lee, C. K.: Global patterns and drivers of leaf photosynthetic capacity: The relative importance of environmental factors and evolutionary history, Global Ecol. Biogeogr., 32, 668-682, https://doi.org/10.1111/geb.13660, 2023.

Zha, J. and Zhuang, Q.: Quantifying the role of moss in terrestrial ecosystem carbon dynamics in northern high latitudes, Biogeosciences, 18, 6245-6269, https://doi.org/10.5194/bg-18-6245-2021, 2021.

Zhang, Y., Xiao, X., Wu, X., Zhou, S., Zhang, G., Qin, Y., and Dong, J.: A global moderate resolution dataset of gross primary production of vegetation for 2000–2016, Sci. Data, 4, 170165, https://doi.org/10.1038/sdata.2017.165, 2017.